Pattern Anal Applic (2014) 17:1–15
DOI 10.1007/s10044-013-0352-8

SURVEY

Reviewing, selecting and evaluating features in distinguishing fine changes of global texture

B. Ortiz-Jaramillo · S. A. Orjuela-Vargas · L. Van-Langenhove · C. G. Castellanos-Dominguez · W. Philips

Received: 14 November 2012 / Accepted: 3 October 2013 / Published online: 19 October 2013

Abstract The evaluation of appearance parameters is critical for quality assurance purposes when determining lifetime and/or beauty of textile products. Practical evaluations of appearance are often performed by human visual inspection, which is repetitive, exhausting, unreliable and costly. Thus, computerized automatic visual inspection has been used to alleviate those problems. Several papers have proposed objective mechanisms for quality inspection mostly using texture analysis approaches which are often not robust enough. One of the main issues for robustness of texture analysis approaches is the capability of distinguishing between similar textures. In this paper, we review, select and evaluate texture analysis approaches for distinguishing fine changes of global texture in degradation of textile floor coverings. As a result, we found that the power spectrum, local binary patterns, the texture spectrum, Gaussian Markov random fields, autoregressive models and the pseudo-Wigner distribution provide good descriptors for measuring fine changes of global texture. That is, those features can be used as starting point in applications involving fine changes of global texture, as well as a basis for the development of new methods.

B. Ortiz-Jaramillo (✉) · W. Philips
Universiteit Gent, iMinds, IPI, St-Pietersnieuwstraat 41, 9000 Gent, Belgium
e-mail: bortiz@telin.ugent.be

S. A. Orjuela-Vargas
Universidad Antonio Nariño, GEPRO, Bogotá, Colombia

B. Ortiz-Jaramillo · C. G. Castellanos-Dominguez
Universidad Nacional de Colombia, SPRG, Bogotá, Colombia

L. Van-Langenhove
Universiteit Gent, De vakgroep Textielkunde, Gent, Belgium

Keywords Appearance retention in floor coverings · Appearance retention in textiles · Fine changes of global texture · Multiple regression analysis · Quality inspection · Texture analysis

1 Introduction

The lifetime and/or beauty of textile products are closely related to the surface appearance [1]. Therefore, the evaluation of appearance parameters is critical for quality assurance purposes when determining lifetime and/or beauty of textile products. The appearance evaluation consists of visually identifying categorized deviations from a reference in textile material surfaces. Particularly, standards for evaluating appearance retention of textile floor coverings are defined in terms of samples exhibiting transitional degrees of degradation related to daily exposure. Usually, practical evaluation is performed by certified experts who compare the standard samples to a test specimen, termed visual inspection. During the evaluation, samples of the original appearance are rated 5, while samples of the changes range from 1 to 4.5 in steps of 0.5 or 1.0 (according with the standard), called *wear labels*. Thus, rate 1 indicates severe wear, whereas a 4.5 rate represents a little change in appearance. Generally, the visual inspection procedure is repetitive, exhausting, unreliable and costly [2]. Therefore, manufacturers are interested in a more objective system, which can be developed using computer vision technologies.

Recently, automatic visual inspection had been used for automatic quality inspection of textile products, mainly, for recognizing defects [3]. Particularly, computer vision technologies had proved to be highly relevant, providing objective measurements of relevant visual attributes related

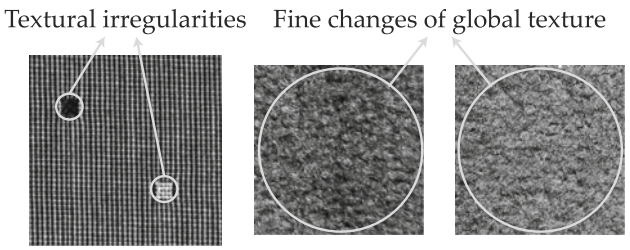

Fig. 1 Comparison between textural irregularities and fine changes of global texture. Texture irregularities are shown as local deviation of texture. Fine changes of global texture are represented by two equal textures with small variation due to wear. *Left image* textile sample exhibiting two defects. *Middle image* cut/frisé textile floor covering with is original appearance. *Right image* cut/frisé textile floor covering after some degree of wear

to the product under inspection [4]. In this regard, several papers consider to automate the quality inspection of textile surfaces using texture analysis approaches [5–10].

Based on computer vision, the quality inspection using texture analysis can be conducted by the following two approaches: (1) using local textural irregularities, in which the main concern is to detect local deviation of texture (Fig. 1 left side); (2) using the fine changes of global texture (FCGT), where texture local patterns do not exhibit abnormalities (Fig. 1 right side). FCGT approach has been largely neglected until recently [8], however, several works dealing with FCGT had been developed, for example [5, 9, 11–13]. Yet, there are no surveys in the literature concerning the evaluation of the FCGT descriptors, in terms of their suitability for implementing the automatic visual inspection.

The aim of this paper is to review, select and evaluate several texture analysis descriptors for distinguishing FCGT, taking advantage of the nature of degradation present on the surface of textile floor coverings. In the beginning, we conduct a review of texture analysis descriptors for evaluating FCGT in textiles. Then based on multiple regression analysis, we propose a methodology for feature selection, in terms of distinguishing FCGT. Obtained findings show that the power spectrum, local binary patterns, the texture spectrum, Gaussian Markov random fields, autoregressive models and the pseudo-Wigner distribution provide good descriptors in measuring FCGT due to degradation in textile floor coverings. That is, those features can be used as starting point in applications involving FCGT, as well as a basis for the development of new methods.

This work is organized as follows: in Sect. 2, current approaches dealing with inspection applications in textiles are discussed. Afterwards, we provide an explanation of multiple regression analysis which is used as framework for feature selection in distinguishing FCGT. Later, Sect. 3 shows the database and the parameters selected for validating our tests. Thereafter, in Sect. 4, we discuss the results obtained in our particular case of study. Finally, in Sect. 5, conclusions and future work are drawn.

2 Materials and methods

In this Section, we discuss current researches dealing with inspection applications of textiles in which FCGT is evaluated. Also, we provide an explanation concerning multiple regression analysis, which is used as framework for feature selection. Afterwards, the proposed methodology for feature selection in distinguishing FCGT is explained.

2.1 Texture analysis approaches and techniques

The aim of this Section is to review the state of art in texture analysis and its applications relating to textile appearance evaluation. Nonetheless, it is not practical to provide an exhaustive overview of all texture analysis techniques. In this section, we present only those techniques in which deviations of texture from original are evaluated. Particularly, we narrow the set of techniques by considering the following applications: (1) roughness measurement, (2) wrinkling evaluation, (3) seam puckering assessment, (4) pilling assessment and (5) appearance retention in floor coverings. Among the most commonly used techniques in appearance evaluation of textiles are the following: co-occurrence matrices [5, 14, 15], filter bank decomposition [16–18], fractal dimension [1, 6, 10], gray level differences [19], gray value histogram analysis [11], the power spectrum [20–23], the Radon transform [24], spatial gray level dependences [25], wavelet analysis [7, 26, 27], Gaussian models [28] and the Wigner distribution [29]. For evaluating small changes in texture, however, the Radon transform is discarded because it can only identify dominant texture and not the small changes we are interested in [3]. Likewise, the fractal approach is discarded since the images under consideration may have the same fractal dimension, while looking completely different [8], which is a disadvantage for identifying small changes in global texture. The remaining techniques that are explained thoroughly in the following paragraphs are organized according to the classical categories, namely, techniques based on statistics, structural primitives, filtering, and models [3, 8].

2.1.1 Techniques based on statistics

These techniques are used to measure the spatial distribution of gray values at specific relative pixel positions [3, 8] and are applied in tasks such as texture analysis, image segmentation, texture classification, defect detection, wear

evaluation, among others [9, 30, 31]. The most popular techniques in this category are described in the following paragraphs.

Autocorrelation function two different textures can be distinguished by evaluating differences in their regularity or fineness presented in the image. One way of measuring these kind of differences is by computing and comparing the autocorrelation function in both textures [32]. The autocorrelation function has been used in several applications such as fabric analysis, macro-texture analysis, estimation of deformation, among others [33–35]. The autocorrelation function of a given image X can be defined as: $\rho = \mathcal{F}^{-1}\{\mathcal{F}\{X\}\mathcal{F}\{X^*\}\}/e$, where $e = \sum_{x=1}^{N}\sum_{y=1}^{M}X^2(x, y)$ is the energy of X, X^* is the complex conjugate of X, $\mathcal{F}\{\cdot\}$ and $\mathcal{F}^{-1}\{\cdot\}$ are the direct and inverse discrete Fourier transform (FT), respectively. Practical algorithms approximate the autocorrelation function using a polynomial $\rho(x, y) \approx a_1x^2 + a_2y^2 + a_3xy + a_4x + a_5y + a_6$, of degree 2 where x and y are the cartesian coordinates [32]. In the present paper, the parameters of the polynomial are used to characterize the image.

Co-occurrence matrix it is one of the most well known texture analysis techniques [3, 36], particularly, in surface flaw detection [5, 12]. The co-occurrence matrix is a matrix of relative frequencies $P(g_1, g_2|(i,j))$, where g_1 and g_2 are gray level values of two disjoint pixels separated by a displacement (i, j). The number of occurrences of g_1 and g_2, separated by the vector (i, j), contributes to the (g_1, g_2)th entry in the matrix of relative frequencies. To characterize those matrices we extract the following parameters: energy, entropy, contrast, homogeneity and correlation [36, 37].

Histograms of sum and difference this technique has proved to be nearly as powerful as the co-occurrence matrices for texture discrimination but exhibiting lower computational cost [38]. Also, it shows a significant capacity to measure visually perceivable qualities of texture [39]. The non-normalized sum and difference of an image X of size $N \times M$ with itself displaced by vector (i, j), are defined as: $S(x, y) = X(x, y) + X(x + i, y + j)$ and $D(x, y) = X(x, y) - X(x + i, y + j)$, respectively. Usually, the following parameters are extracted from the histograms of S and D to characterize the image: mean, energy, correlation, entropy, contrast and homogeneity [38].

Texture spectrum and Local Binary Patterns (LBP) the key concept of these methods is the computation of the relative intensity relations between the pixels in a small neighborhood and not on their absolute intensity values. The LBP is a widely used texture descriptor including a wide range of extensions [40]. The texture spectrum and LBP are computed as follows: from a given set of pixels in Fig. 2, it is possible to compute a texture code, $g_{3^k} = \sum_{k=0}^{7} T_1(g_k - g_c)3^k$ for the texture spectrum and $g_{2^k} = \sum_{k=0}^{7} T_2(g_k - g_c)2^k$ for the LBP, where

$$T_1(x) = \begin{cases} 0, & \text{if } x<0 \\ 1, & \text{if } x=0 \\ 2, & \text{if } x>0 \end{cases}, \quad T_2(x) = \begin{cases} 0, & \text{if } x<0 \\ 1, & \text{if } x\geq 0 \end{cases},$$

then texture units are grouped into a histogram to characterize the image.

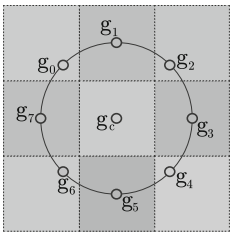

Fig. 2 Pixel set distributed within a circular symmetric neighbor. Here, a eight *circularly* symmetric neighbor

2.1.2 Techniques based on structural primitives

From the structural point of view, texture is characterized by primitives and spatial arrangement of those primitives [3, 8, 36]. Usually, texture primitives are collected from a number of different samples assuming that texture is regular. Within the textile defect detection framework, for instance, it is possible to cover the range of variations by extracting textural primitives from non-defective samples [8]. Then, any variation from the textural primitives is classified as a defective sample. Therefore, these kind of algorithms are limited in discrimination power except for regular textures [36]. When evaluating texture appearance due to degradation of textiles at local small scales, the resulting textures may not exhibit regular patterns. This aspect makes techniques based on structural primitives impractical for evaluating texture appearance due to degradation.

2.1.3 Techniques based on filtering

Most of the techniques based on filtering apply linear transformations or filter bank decomposition, followed by computing some energy measures [3, 8, 36, 37]. Particularly, the spectral histogram is widely used as descriptor in texture analysis applications [41]. The construction of the spectral histogram is illustrated in Fig. 3, where $h_0, \ldots, h_{k-1}$ are image filters, $X_0, \ldots, X_{k-1}$ are the images after filtering and $f_0, \ldots, f_{k-1}$ are the histograms of those images. Spectral histograms have been used in several texture analysis tasks [41, 42]. We use the spectral histogram for characterizing an image after applying one of the following signal decomposition methods: eigenfilters, Gabor filters, the Gaussian pyramid, the Laplacian pyramid, measures of

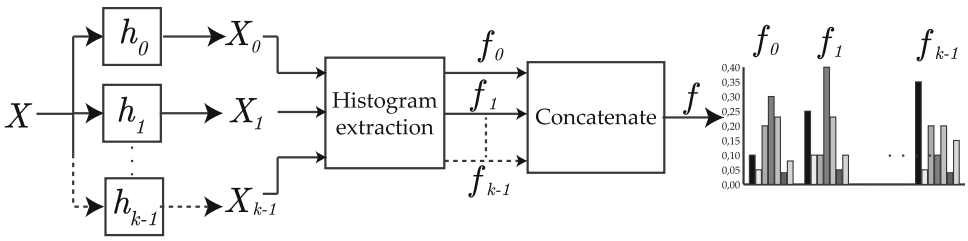

Fig. 3 Spectral *histogram* feature extraction for an image decomposed in k components

Laws, the steerable pyramid, the wavelet transform and the pseudo-Wigner distribution. Those signal decomposition methods are detailed in the following paragraphs.

Power spectrum the FT is used in a wide range of applications, such as image analysis, image filtering, image reconstruction, image compression and the texture analysis. From the power spectrum of the FT, it is possible to extract several descriptors (for more detail see [3, 32]). Particularly, a set of wedge and ring filters have been suggested, assuming that texture is discriminant in spatial frequency and orientation [3, 37, 43]. In this paper, we use the set of dyadic filters proposed in [43]. After applying that set of filters we extract ten energy measures characterizing coarseness and directionality of the texture.

Eigenfilters The ability to incorporate various spatial and spatial-frequency constraints make eigenfilters an useful tool for signal analysis and synthesis [44], as well as in a variety of applications [44, 45]. The eigenfilters are computed as follows: Suppose that d overlapping windows of size $W \times W$ (usually window size is 3×3) are extracted from an image. After vectorizing those windows, it is possible to arrange them as row entries of a matrix E of size $d \times W^2$. Afterwards, the covariance matrix is computed from the new matrix of data as $B = E^T E$. Then, a singular value decomposition over the covariance matrix B is performed to obtain W^2 eigenvectors. Usually, those eigenvectors are used as filters to perform a filter bank decomposition that results in a set of images. Lastly, the spectral histogram is computed from those images to characterize the texture.

Gabor filters Gabor filtering allows imaging with optimal joint localization in the spatial–spatial/frequency domain [3, 37, 42, 46]. Also, it is widely used for characterizing the human vision system [46, 47]. Hence, this technique should be appropriate for identifying and quantifying the degree of wear in a textile floor covering using image analysis. Mathematically, a two-dimensional Gabor function $g(x, y)$ is defined as [46],

$$g(x,y) = \frac{1}{2\pi\sigma_x\sigma_y}\exp\left(-\frac{1}{2}\left(\frac{x^2}{\sigma_x^2}+\frac{y^2}{\sigma_y^2}\right)+2\pi j u_0 x\right) \qquad (1)$$

Here, σ_x and σ_y characterize the band width of the filter centered at the point $(u_0,0)$ in the spatial/frequency domain. From Eq. (1) it is possible to generate a set of Gabor functions by appropriate dilations and rotations, i.e.,

$$\begin{aligned} g_{m,n} &= a^{-m} g(x', y'), \quad a > 1, \quad m, n \in \mathbb{Z} \\ x' &= a^{-m}(x\cos(\theta) + y\sin(\theta)) \\ y' &= a^{-m}(-x\sin(\theta) + y\cos(\theta)) \end{aligned}$$

where $\theta = n\pi/K$, with $n = 0, \ldots, K-1$,ê and K is the total number of orientations. Here a^{-m}, with $m = 0, \ldots, L-1$, is the scale parameter, where L is the number of scales. Usually, that set of filters is used for performing a filter bank decomposition that results in a set of images. Afterwards, the spectral histogram is computed from those images to characterize the texture.

Gaussian pyramid the Gaussian pyramid is one of the simplest multi-scale representations on image processing. This kind of pyramid is created using Gaussian filters with increasing spatial resolution. A Gaussian pyramid consists of low-pass filtered and downsampled images of the original image [48]. In this paper the spectral histogram is extracted from those low-pass filtered and downsampled images to characterize the texture.

Laplacian pyramid the laplacian pyramid is very similar to the laplacian of Gaussian and the difference of Gaussian filters [48]. It is also a multi-scale technique that is more desirable than a single-scale technique. Also, the laplacian pyramid has been used in several texture analysis applications [49, 50]. The laplacian pyramid consists of a sequence of differences between two consecutive levels of the Gaussian pyramid [48], i.e., $X_{j+1} = X_j - \widetilde{X}_j$, where X_j is the image X at the jth level and $\widetilde{X}_j$ is the image X at the jth level after Gaussian filtering. Here, we compute the spectral histogram from that sequence of differences to characterize the image under analysis.

Measures of laws Laws filters are considered as one of the first filtering approaches in texture analysis, presented by Laws [51]. This technique has been used and referenced very often in the texture analysis field [52, 53]. Laws suggested five separable filter masks for characterizing an image. By convolving an image across rows and columns with that set of masks, 25 images characterizing the image under analysis are obtained. Afterwards, a non-linear windowing operation is applied as proposed in [51]. Finally, images representing the same information are

combined to obtain a set of 14 images as discussed in [51]. From those images, the spectral histogram is extracted to characterize the texture.

Steerable pyramid the steerable pyramid incorporates a multi-orientation image decomposition to a multi-scale method. In this decomposition, an image is divided into a collection of levels localized in both scale and orientation [54]. This technique has been proved to be successful in several texture analysis tasks [55, 56]. In general, this pyramid is obtained using Gaussian filters, downsampled images and first derivatives of those images. Thus, an image at the jth scale in direction θ is defined as $X_{j,\theta} = \cos(\theta)X_{j,x} + \sin(\theta)X_{j,y}$ where $j = 0,\ldots,J-1$, $X_{j,x}$ and $X_{j,y}$ are the scale, first derivative in x and y direction, respectively [55, 56]. Finally, to obtain the steerable pyramid, it is necessary to repeat the above procedure for several angles $\theta_0,\ldots,\theta_k$, resulting in a set of images. From the images representing scale and orientation, the spectral histogram is extracted to characterize the texture.

Wavelet transform the wavelet transform has been extensively used in texture analysis [41, 57]. Particularly, the application of the discrete wavelet transform (DWT) for texture identification has received considerable attention in the literature. The DWT is seen as a filter bank decomposition of an image using a low-pass and high-pass filters that results in a set of images [57]. Afterwards, the spectral histogram is computed from those images to characterize the texture.

Wigner distribution in recent years, the Wigner distribution (WD) has become one of the most popular techniques to describe local joint distribution in image processing tasks [29, 58]. Usually, the computation of the 2D WD is carried out numerically when the available data is discrete. This numerical approximation is termed as pseudo-Wigner distribution (PWD). The PWD of a two-dimensional discrete function is defined as follows:

$$\begin{aligned}\mathrm{PWD}\{X\}(x,y,u,v) = \sum_{i=-W/2}^{W/2}\sum_{j=-W/2}^{W/2} h_s(i,j) \sum_{k=-W/2}^{W/2}\sum_{l=-W/2}^{W/2} \\ h_f(k,l)X(x+k+i,y+l+j) \\ X^*(x+k-i,y+l-j) \\ \exp(-2\jmath(iu+jv))\end{aligned}$$

where h_s, h_f are two smoothing windows of size $W \times W$ (usually window size is 5×5) and X^* is the complex conjugate of X. The result of applying the $\mathrm{PWD}\{\cdot\}$ is a set of W^2 images that are used to characterize the spatial/spatial-frequency distribution of an image. Here, we compute the spectral histogram from those images to characterize the image under analysis.

Table 1 Summary of the used techniques

Abbreviation	Technique
FFT	Power spectrum
LBP	Local binary patterns
TSU	Texture spectrum
MRF	Gaussian Markov random field
AR	Autoregressive models
PWD	Wigner distribution
AF	Autocorrelation function
IH	Image Histogram
GP	Gaussian pyramid
GF	Gabor filters
CP	Co-occurrence matrix
LP	Laplacian pyramid
DWT	Wavelet
SDH	Histograms of Sum and diff.
ML	Measures of Laws
SP	Steerable pyramid
EF	Eigenfilter

2.1.4 Techniques based on models

these kind of techniques uses stochastic or generative models to represent images. Then, the estimated model parameters are used to characterize the image [3].

Autoregressive models autoregressive (AR) models exploit the linear dependency between image pixels [8, 37, 59]. The AR models have been applied in several tasks such as texture synthesis, texture segmentation and texture classification [59, 60]. Mathematically, a two-dimensional AR model is defined as the linear combination of the surrounding neighbors of a central point [59]. The AR model for the central pixel in Fig. 2 is given by $\hat{g}_c = \sum_{k=0}^{7} a_k g_k$, where a_k for $k = 0,\ldots,7$ are the parameters of the model to be estimated. Particularly, this method is called circular autoregressive model [59]. If overlapped circular neighbors are taken, the above statement can be generalize as

$$\widehat{X}(x,y) = \sum_{i=-1}^{1}\sum_{j=-1}^{1} a(i,j)X(x+i,y+j).$$

Usually, the set of parameters are estimated using the least squares method. In this work, that parameters are used to characterize the texture.

Gaussian Markov random fields (GMRF) Markov random fields (MRF) have been very popular for modeling images. They have been applied in several tasks such as image segmentation, texture synthesis and classification [61–63]. Also, the MRF provides means to capture the local information in an image [3, 36]. Particularly, the parameters of GMRF, unlike to other MRF extensions, can

be computed efficiently. Furthermore, GMRF have proved to be suitable for image classification and defect detection [64]. In this paper, the GMRF for the third order Markov neighbors is computed as discussed in [64]. The GMRF model is defined by the following formula:

$$p(X(x,y)|X(x+i,y+j),(i,j)\in[-2,2]) = \frac{1}{\sqrt{2\pi\sigma^2}}\exp\left(-\frac{1}{2\sigma^2}\left(X(x,y)-\sum_{l=1}^{6}\alpha_l S_{x,y,l}\right)^2\right),$$

where $S_{x,y,l}$ for $l = 1,\ldots,6$ are defined as follows:

$$\begin{aligned} S_{x,y,1} &= X(x-1,y)+X(x+1,y)\\ S_{x,y,2} &= X(x,y-1)+X(x,y+1)\\ S_{x,y,3} &= X(x-2,y)+X(x+2,y)\\ S_{x,y,5} &= X(x-1,y-1)+X(x+1,y+1)\\ S_{x,y,6} &= X(x+1,y-1)+X(x-1,y+1) \end{aligned}$$

Here, seven parameters are estimated ($\{\alpha_1,\ldots,\alpha_6,\sigma\}$) characterizing the texture under analysis. Those parameters are estimated by least squares method. Table 1 summarizes the techniques used in this paper.

2.2 Feature selection using multiple regression analysis

Before giving details about the proposed methodology for feature selection (in statistics: selection of variables), it is necessary to introduce some key concepts in the field of multiple regression analysis. Multiple regression is a method used to model the relationship between a variable provided by a system or an expert (in statistics: the response variable) and one or more input variables provided by measuring physical magnitudes (in statistics: the predictor variables). A linear model is defined as $\boldsymbol{c} = D\boldsymbol{\beta} + \boldsymbol{\epsilon}$, where $\boldsymbol{c} \in \mathbb{R}^{n\times 1}, D \in \mathbb{R}^{n\times p}, \boldsymbol{\beta} \in \mathbb{R}^{p\times 1}$ and $\boldsymbol{\epsilon} \in \mathbb{R}^{n\times 1}$ are the response variable, predictor variables, unknown parameters and error associated to the model, respectively.

There are two common used measures for determining the success of the linear model. One is the coefficient of determination which is defined as

$$R^2 = \frac{\hat{\boldsymbol{\beta}}^T D^T \boldsymbol{c} - (\sum \boldsymbol{c})^2/\boldsymbol{n}}{\boldsymbol{c}^T\boldsymbol{c} - (\sum \boldsymbol{c})^2/\boldsymbol{n}}.$$

The second is the partial coefficient of determination which is defined as

$$\rho^2_{\boldsymbol{c},\boldsymbol{d}_{\bullet j}} = \frac{\hat{\beta}_j \boldsymbol{d}^T_{\bullet j}\boldsymbol{c} - (\sum \boldsymbol{c})^2/\boldsymbol{n}}{\boldsymbol{c}^T\boldsymbol{c} - (\sum \boldsymbol{c})^2/\boldsymbol{n}},$$

where $\boldsymbol{d}_{\bullet j}$ and $\hat{\beta}_j$ are the jth predictor variable and estimated parameter, respectively. Here, $\hat{\boldsymbol{\beta}}$ is the least square estimation of $\boldsymbol{\beta}$, i.e., $\hat{\boldsymbol{\beta}} = (D^T D)^{-1}(D^T\boldsymbol{c})$.

The selection of variables is probably the most fundamental and important topic in regression analysis. First, it is necessary to build models with high coefficient of determination between response and predictor variables. Second, it is necessary to select the model with the smallest number of predictor variables for keeping the smallest variance in the estimated parameters. The idea of selecting the <<best>> regression model from a set of predictor variables (features) is to find a balance between goodness of fit versus small variance in parameters [65]. Several studies in the literature have highlighted that including irrelevant predictor variables or features in the model produces overfitting. Also, it is required a high computational cost even with moderate number of predictor variables ($2^p - 1$ models to test, where p is the number of predictor variables or features) [65, 66]. Thereafter, there is the challenge of concluding which model is significantly better than the others [65]. In this field, several approaches have been applied such as standardized parameters, simple correlation, ANOVA, Pratt's measure, decomposition of the coefficient of determination [65, 67]. Particularly, the decomposition of the coefficient of determination proposed by Genizi [67] can be used as framework to design a methodology for selecting features using an orthogonal transformation of D. The construction of the matrix D is explained thoroughly in Sect. 2.3 The main idea of the Genizi approach is that when a set of mutually orthogonal predictors is available, the sum of each partial coefficient of determination is equal to the coefficient of determination. That is, $R^2 = \sum_{j=1}^{p} \rho^2_{\boldsymbol{c},\boldsymbol{d}_{\bullet j}}$. In such case, it is possible to conclude that the most relevant predictor variables or features in the linear model are those variables with greater partial coefficient of determination. However, predictor variables are often non mutually orthogonal. In that case, it is necessary to find an index v_j for $j = 1,\ldots,p$ which holds the condition $R^2 = \sum_{j=1}^{p} v_j$ for non mutually orthogonal variables. That index can be computed using a singular value decomposition of the data correlation matrix as $D^T D = QC^2Q^T$. Thus, each variable has an index representing its relevance in the linear model, which is computed as:

$$v_j = \sum_{k=1}^{p} a^2_{j,k}\gamma^2_k, \tag{2}$$

where $a_{j,k}$ is the (j,k)th element of the matrix $A = QCQ^T$ and γ_k is the kth element of the vector $\boldsymbol{\gamma} = AD^{-1}\boldsymbol{c}$ as discussed in [47, 67]. Using v indexes, it is possible to conclude that the most relevant predictor variables or features in the linear model are those variables with greater v index [47]. Then, a simple backward elimination or forward selection can be performed using as elimination or addition criteria the v index, respectively. Finally, the <<best>>

model is selected by finding a compromise between the coefficient of determination and the number of predictor variables or features. This procedure ensures that the <<best>> model is selected by testing only p models instead of $2^p - 1$ models [47, 67].

2.3 Proposed methodology for feature selection in distinguishing fine changes of global texture

Figure 4 shows the proposed methodology for variable selection (feature selection) using multiple regression analysis in distinguishing FCGT due to degradation on textile floor coverings. This methodology was based on recent advances in which the appearance retention of floor coverings is measured [9, 12, 13]. First at all, the i-th image X_i is preprocessed and divided into two sub-images $X_{w,i}$ (worn area) and $X_{u,i}$ (unworn area). This procedure is explained in Sect. 3 Then, texture descriptors are extracted independently from each image, termed $\zeta_{w,i}$ (texture descriptors extracted from a worn area of the image) and $\zeta_{u,i}$ (texture descriptors extracted from an unworn area of the image). Here, $\zeta_{w,i}$ and $\zeta_{u,i}$ are the parameters and histograms explained in Sect. 2.1 computed from worn and unworn areas, respectively. It means that $\zeta_{w,i}$ and $\zeta_{u,i}$ are set of vectors, in which, each vector represents a descriptor extracted using a particular technique. Afterwards, a dissimilarity measure between each pair of vectors is computed, i.e., $d(\zeta_{w,i}, \zeta_{u,i}) = \boldsymbol{d}_{i,\bullet}$, where $d(\cdot,\cdot)$ is an appropriate metric or pseudo metric according to the nature of the descriptor. In this work, with the purpose of measuring differences between worn and unworn samples, the Euclidean distance and the symmetrized adaptation of the Kullback-Leibler divergence are used.

On the one hand, the Euclidean distance was selected to measure differences in the following techniques: AF, AR, CP, SDH, FFT and MRF. That distance was selected for measuring differences in those techniques because it is probably the most common chosen type of distance due to its simplicity. Also, the Euclidean distance can be used to model numerous natural facts of the human-scale world and most of the powerful image recognition techniques make use of it [68]. On the other hand, we use the symmetrized adaptation of the Kullback-Leibler divergence in the following techniques: IH, TSU, LBP and spectral histograms extracted from: EF, GF, GP, LP, ML, SP, DWT and PWD. This divergence is used to measure differences in the above techniques because those generate a histogram and the symmetrized adaptation of the Kullback-Leibler divergence has proved to be very accurate in measuring differences between histograms. Also, it has proved to be very suitable for texture analysis applications [9, 32, 41, 42].

Here, we consider those differences as predictor variables or features of the linear model. Then, we define $\boldsymbol{d}_{\bullet,j} \in \mathbb{R}^{n\times 1}$ as the jth column of the matrix D where each entry is a difference obtained from worn and unworn areas for the jth descriptor. Also, we define each row of D ($\boldsymbol{d}_{i,\bullet} \in \mathbb{R}^{1\times p}$) as the differences obtained from worn and unworn areas for the ith sample. It means, each entry of the matrix $D = [d_{i,j}]_{n\times p}$ represents a descriptor difference between worn and unworn areas using the jth technique on the ith sample.

Finally, given the evaluation of the experts, termed wear labels $\boldsymbol{c}$, and computing the matrix of differences D (descriptor variables or features), we obtain the matrix A and vector $\boldsymbol{\gamma}$. Afterwards, v index is obtained for each predictor variable as is shown in Eq. (2). Then, the model is selected by performing a backward elimination or forward selection using as elimination or addition criteria the v indexes. Finally, predictor variables are added or removed as discussed in Sect. 2.2

3 Experimental set-up

3.1 Database

We use two databases, each one composed with samples of wear with grades in steps of 0.5 from 1.0 to 4.5. Also, we have an extra database which only possesses four samples of wear from 1.0 to 4.0 in steps of 1.0.

The first set of images is composed of scanned printed images, using an office scanner, from the CRI standard

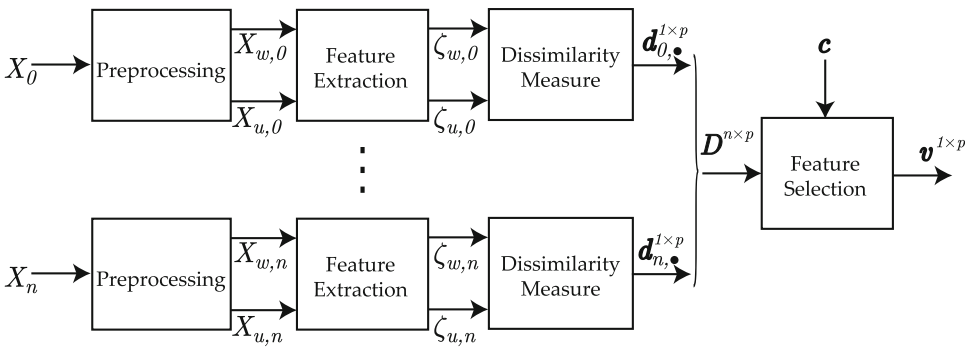

Fig. 4 Proposed methodology for feature selection in distinguishing fine changes of global texture

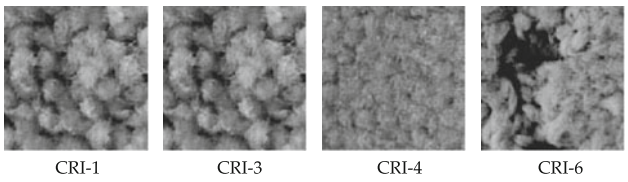

Fig. 5 Textures evaluated from the CRI standard

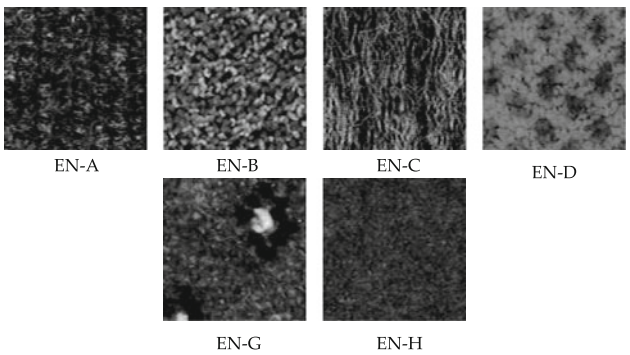

Fig. 6 Textures evaluated from the `EN1471` standard

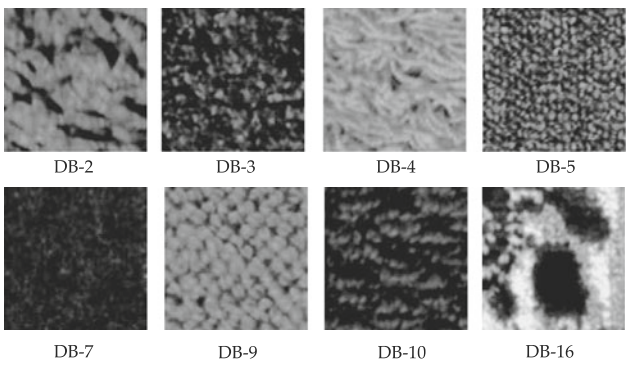

Fig. 7 Textures evaluated from the Ghent University—Textile Department DB

photo set. The CRI references include texture types with loop (CRI-3), cut (CRI-1 and CRI-4) and tip-sheared (CRI-6) piles, see Fig. 5. To keep the relevant characteristics in the scanned images we used a resolution of 7.8 pixels per milliliter. Each reference contains photographs corresponding to eight wear degrees from 1.0 to 4.5 in steps of 0.5. Also, in the same photograph, the original texture of the floor covering is included. Each printed photograph was digitized in a 2,300 × 1,100 pixels image [9].

The second set of images is composed of photographs of physical samples from loop (EN-A), cut/frisé (EN-B), woven cut (EN-G), and cut/tufted (EN-C, EN-D and EN-H) piles from the `EN1471` standard, see Fig. 6. In these sets, wear degrees were photographed at 30 *cm* with a progressive `3CCD Sony` camera model `DXC-9100 P` using a `Sony` macro lens model `VCL-707BXM`. We took

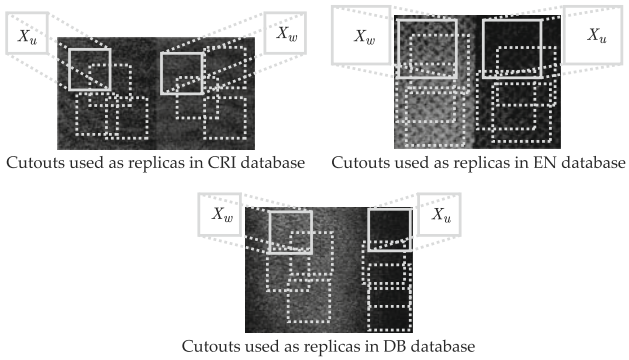

Fig. 8 Cropping procedure. Cut outs of 400 × 400 used as replicas

photographs of size of 720 × 576 pixels corresponding to 18 × 14.5 cm^2. This offers a resolution of 4 pixels per milliliter, which is proved to be sufficient for describing the wear of this references. Each reference contains photographs corresponding to four wear degrees from 1.0 to 4.0 in steps of 1.0. Also, in the same photograph, the original texture of the floor covering is included [9].

In the third database, the wear degrees were assessed by three inspectors of the textile Department of Ghent University, in collaboration with the textile floor covering company LANO. The set is composed of one high/low loop (DB-10), two loops (DB-5 and DB-9), one cut (DB-7), one cut design (DB-16), one frizé (DB-3) and two types of shaggy (DB-2 and DB-4) piles, see Fig. 7. Each physical sample corresponds to the eight wear degrees from 1.0 to 4.5 in steps of 0.5. Also, in the same sample, the original texture of the floor covering is preserved. The physical samples were photographed at 30 *cm* with a progressive `3CCD Sony` camera model `DXC-9100 P` using a `Sony` macro lens model `VCL-707BXM`. We took photographs of size of 720 × 576 pixels corresponding to 18 × 14.5 cm^2. This offers a resolution of four pixels per millimeter [13].

3.2 Preprocessing

The preprocessing stage is performed in two steps. The first step involves a cropping procedure which is shown in Fig. 8. This cropping procedure is performed by extracting random cutouts from either the part of the original or the part with the appearance change. We used this cropping procedure with the purpose of increasing the number of samples in the experiment (we analyze many cropped regions instead of one large image). Thus, using more samples it is possible to reduce the variance of the results for providing more accurate conclusions. The second step involves gray scale conversion. As standards for evaluating appearance changes judge color and surface changes independently, our analysis is based on gray scale images.

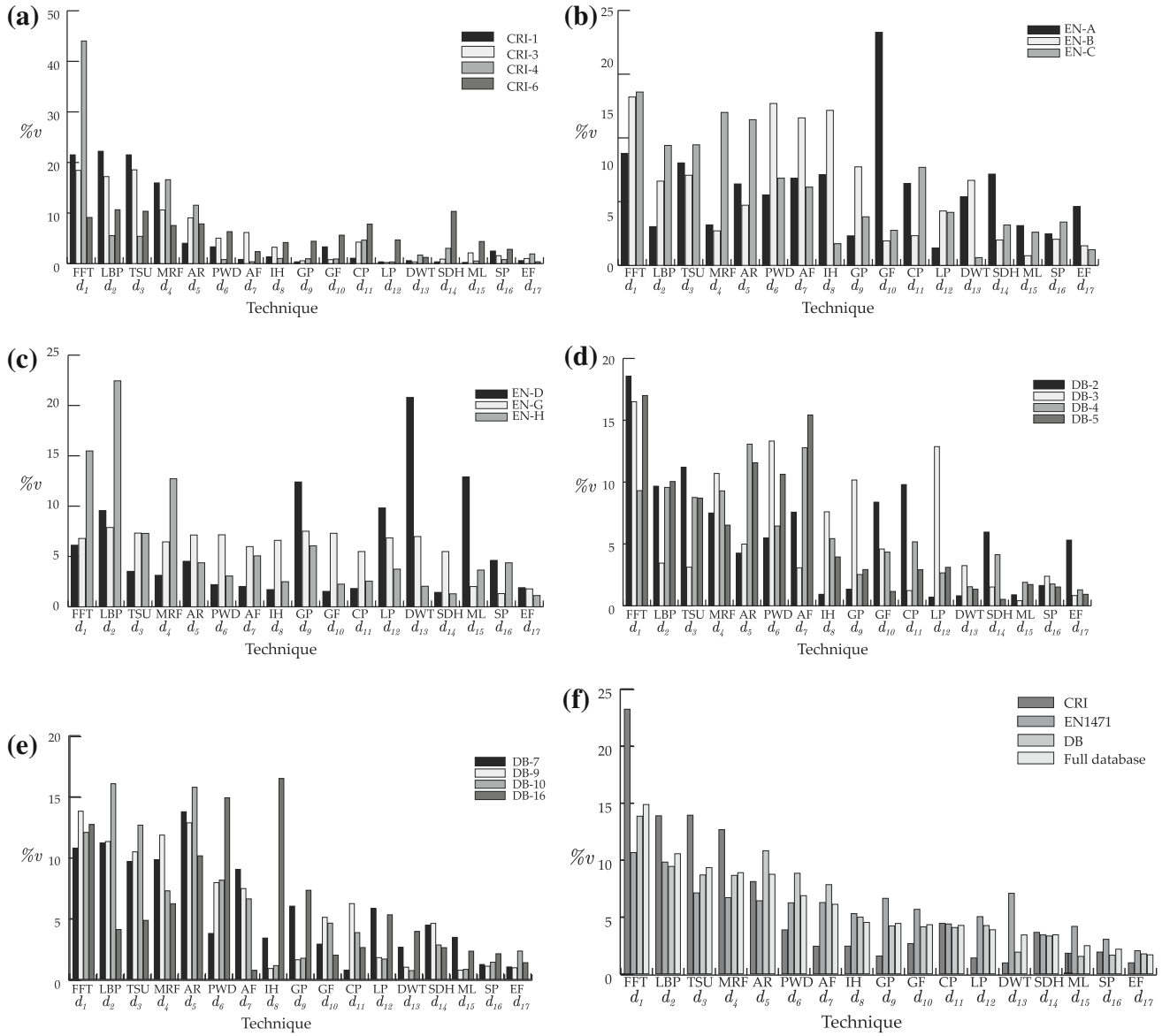

Fig. 9 Relevance of the predictor variables using the proposed methodology for the three databases. *%v* is the relevance of the variable for the linear model in a range of [0−100] %. **a** CRI database, **b** `EN1471` database part 1, **c** `EN1471` database part 2, **d** DB database part 1, **e** DB database part 2, **f** Mean values

3.3 Parameter selection for the techniques

In this paragraph, we summarize the parameters and descriptors used for each technique described in Sect. 2.1 (1) In the *autocorrelation function* technique, we use the parametric model explained in [32]. Thereby, the texture descriptor is represented by the coefficients of a two-dimensional second-order polynomial. (2) In the *co-occurrence matrix* technique, we extracted from every matrix P, with displacement (i, j), the following measures: energy, entropy, contrast, homogeneity and correlation [36, 37]. Also, we used the displacements suggested in [37]. (3) From the *histograms of sum and difference* we computed mean, energy, correlation, entropy, contrast and homogeneity [38]. In our experiments we used the same displacement vectors used in *co-occurrence matrix*. (4) In the *texture spectrum and the LBP*, the texture units were grouped into a histogram to extract the texture descriptor [40]. (5) The parameters estimated in *AR and GMRF models* are used as local image descriptors.

(6) In the *power spectrum*, a set of wedge and ring filters proposed by Weszka et. al. [43] were used. (7) From *eigenfilters, Laplacian pyramid, Laws filters, steerable pyramid and Wigner distribution*, the spectral histogram explained in Sect. 2.1 is extracted as texture descriptor. (8) In the case of *Gabor filters*, we used the configuration

Table 2 Post hoc test based on Friedman test

Median rank		FFT	LBP	TSU	MRF	AR	PWD	AF	IH	GP	GF	CP	LP	DWT	SDH	ML	SP	EF
3	FFT	–	←	←	←	←	←	←	←	←	←	←	←	←	←	←	←	←
4	LBP	0.21	–	←	←	←	←	←	←	←	←	←	←	←	←	←	←	←
5	TSU	1.00	0.44	–	←	=	←	←	←	←	←	←	←	←	←	←	←	←
6	MRF	1.00	0.53	0.58	–	↑	←	←	←	←	←	←	←	←	←	←	←	←
5	AR	0.40	0.59	0.96	0.45	–	←	←	←	←	←	←	←	←	←	←	←	←
7	PWD	0.25	0.53	0.26	0.58	0.25	–	←	←	←	←	←	←	←	←	←	←	←
9	AF	0.00	0.03	0.04	0.04	0.05	0.04	–	←	=	←	←	←	←	←	←	←	←
10	IH	0.03	0.04	0.03	0.02	0.03	0.05	0.90	–	←	=	=	←	←	←	←	←	←
9	GP	0.04	0.02	0.05	0.04	0.04	0.03	0.74	1.00	–	←	←	←	←	←	←	←	←
10	GF	0.03	0.03	0.01	0.02	0.03	0.05	1.00	1.00	1.00	–	=	←	←	←	←	←	←
10	CP	0.02	0.02	0.00	0.05	0.02	0.03	1.00	1.00	1.00	1.00	–	←	←	←	←	←	←
11	LP	0.01	0.01	0.03	0.04	0.01	0.04	0.90	1.00	0.24	1.00	1.00	–	←	=	←	←	←
12	DWT	0.01	0.01	0.01	0.03	0.01	0.04	0.45	0.18	0.09	0.97	0.75	1.00	–	↑	←	←	←
11	SDH	0.01	0.01	0.00	0.03	0.01	0.02	0.53	1.00	1.00	1.00	0.36	1.00	1.00	–	←	←	←
13	ML	0.00	0.00	0.01	0.01	0.00	0.01	0.09	0.26	0.07	0.91	0.18	0.45	1.18	0.65	–	=	←
13	SP	0.00	0.00	0.00	0.00	0.00	0.01	0.10	0.77	0.12	1.00	0.19	1.05	0.89	1.00	1.00	–	←
14	EF	0.00	0.00	0.00	0.00	0.00	0.00	0.03	0.11	0.09	0.06	0.00	0.42	0.83	0.13	0.89	0.67	–

Adjusted p values were obtained using Bonferroni–Holm correction for multiple comparisons. In each entry, the direction of the *arrow* indicates which of the two methods (row or column) perform better. The equal sign stands for a tie. Elements below the diagonal are p values. If p values are higher than 0.05, there were no significant differences between the methods. The median rank is a measure of performance, e.g., the ideal performing descriptor should have median rank of 1

proposed by Manjunath and Ma [46] with the purpose of reducing the redundancy presented in the filter bank decomposition. Then, the spectral histogram is also extracted as texture descriptor. (9) In the case of *Gaussian pyramid*, a dyadic scale-space is used because it has proved to be a good and efficient discrete representation of the scale-space [69]. After applying the Gaussian pyramid the spectral histogram is also extracted as texture descriptor. (10) Finally, for wavelet transform, as the evaluation of absolutely all filter banks is beyond of the main scope of this study, we selected the Daubechies 9/7 wavelet because it has been used very often in textural analysis tasks [57]. From this filter bank decomposition the spectral histogram is also extracted as texture descriptor.

4 Results and discussion

Figure 9 shows the relevance of the predictor variables (features) for the corresponding databases in a range of [0–100] %. The percentages are related to the relevance of the predictor variable in distinguishing FCGT due to degradation on textile floor coverings. Figure 9f shows the mean values of v indexes for each database. Taking into account that $R^2 = \sum_{j=1}^{p} v_j$, it is possible to conclude that the first six techniques accounted at least the 70 % of the coefficient of determination. According to those v indexes, the most relevant features or predictor variables are those provided by the power spectrum, local binary patterns, the texture spectrum, Gaussian Markov random fields, autoregressive models and the pseudo-Wigner distribution.

To validate the results obtained by the linear regression methodology, we use the Friedman test and pairwise comparisons as discussed in [70]. Here, the related samples are the performance of the methods measured across the types of textile floor coverings. Using Friedman test, we found that there are statistically significant differences between the techniques (p value = 0.00). To examine where the differences actually occur, we use pairwise comparisons on the different combinations of related groups. Table 2 shows the pairwise comparisons between the techniques evaluated in this paper. From the table, it is possible to conclude that there are no statistically significant differences between FFT, LBP, TSU, MRF, AR and PWD (p values higher than 0.21). Also, from the Table it is possible to conclude that those techniques perform better than the rest of techniques evaluated in this paper (p values lower than 0.05).

Since we are interested in selecting the best model with lower number of variables, we use the methodology presented in Sect. 2.2 using forward selection. In such case, we only have to test the following models: $\boldsymbol{c} = \sum_{j=1}^{k} \beta_j \boldsymbol{d}_{\bullet j}$, where $k = 1, \ldots, p$, β_j and $\boldsymbol{d}_{\bullet,j}$ are the model number, the parameters of a linear model and the descriptors

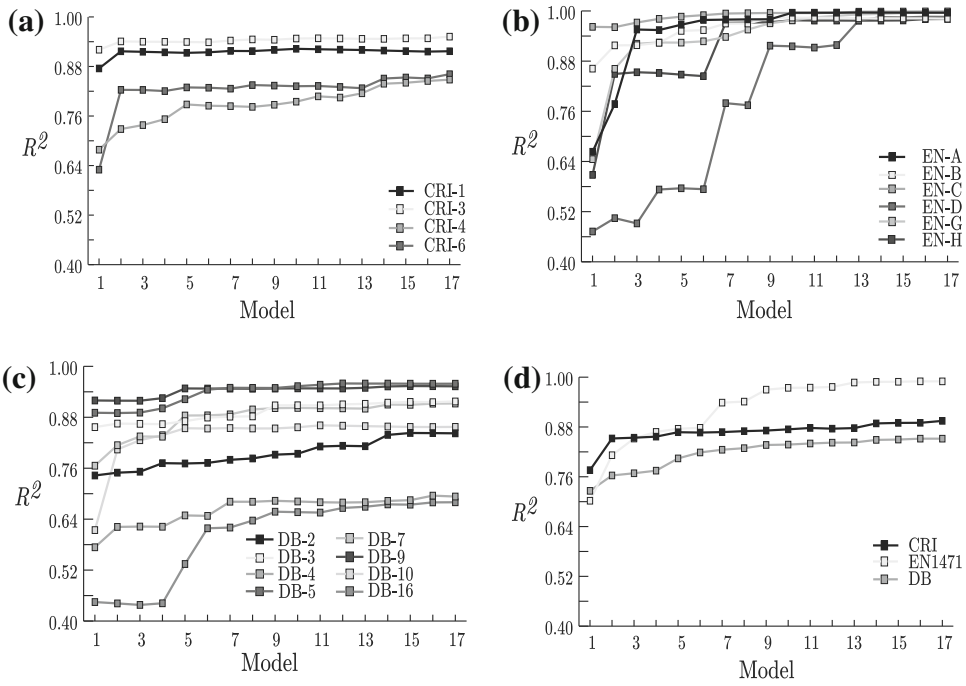

Fig. 10 Model selection using coefficient of determination and the proposed methodology for the three databases. Coefficient of determination per reference versus number of features into the model. **a** CRI database, **b** EN1471 database. **c** DB database, **d** Mean values

enumerated as shown in Fig. 9, respectively. Those models were selected using as variable addition criteria the v indexes in a forward selection algorithm. Coefficients of determination for the corresponding models are presented in Fig. 10 as function of the model number. With these plots, it is possible to identify which models are more suitable for each database. Figure 10d shows the mean coefficient of determination for the corresponding databases. According to those mean values, the model with the higher mean performance and minimum number of variables is the model of order 2 which is consistent with median ranks in Table 2. This model combines those two predictor variables with the higher v index and median rank. Here, the predictor variables (features) with higher v index and median rank are the differences between descriptors in the power spectrum (FFT) and the local binary patterns (LBP), see Fig. 9 and Table 2. Then, we chose as model the linear combination between FFT and LBP, i.e., $\hat{c} = \beta_0 + \beta_1 d_1 + \beta_2 d_2$, where $\hat{c}, d_1, d_2$ and $\beta_i, i = \{0, 1, 2\}$ are automatic assessment, differences between FFT descriptors, differences between LBP descriptors and constants to best fit with human assessment, respectively.

To validate the selected model, we use the leave-one-out cross validation procedure as discussed in [71]. Figures 11–13 show the validation using leave-one-out procedure for the corresponding databases. Each reference is described by an error bar plot representing good of fit of estimation of an incoming sample. The gray strips represent the error accepted by experts, i.e., a labeling error below ± 0.5 [2, 13].

The plot for references CRI-1 and CRI-3 (Fig. 11a, b, respectively) shows an adjusted coefficient of determination over 0.9 and the error of labeling in the worst case scenario is below 0.5 which is within the error interval accepted by experts. The other two plots (Fig. 11c, d) show a lower performance. However, the monotonic behavior instead of a random behavior gives a good indication for developing complementary features in measuring appearance retention in floor coverings. For instance, the reference CRI-6 is a level loop with small repetitive patterns. Usually, the change of pattern definition is very important for measuring the degree of wear in textile floor coverings [13]. Because of that it is necessary to include features capable of measuring the change of pattern definition for performing a better characterization of the textile floor covering.

Figure 12 shows the results for the database EN. From those plots it is possible to conclude that when a labeling error of 1.0 between consecutive wear labels is allowed, the linear combination between features of FFT and LBP is enough for measuring appearance retention in floor coverings. Only one of the models does not fit well (Fig. 12d). In this reference we have also a loop pile with repetitive patterns in which, as was established before, it is very important to measure the change of pattern definition.

Figure 13h, floor covering with cut pile design, shows the worst performance with labeling errors up to 1.5 in the worst case scenario. This fact shows that the methods are not good enough for assessing textile floor coverings with complex patterns. Also, Fig. 13a and c, floor coverings

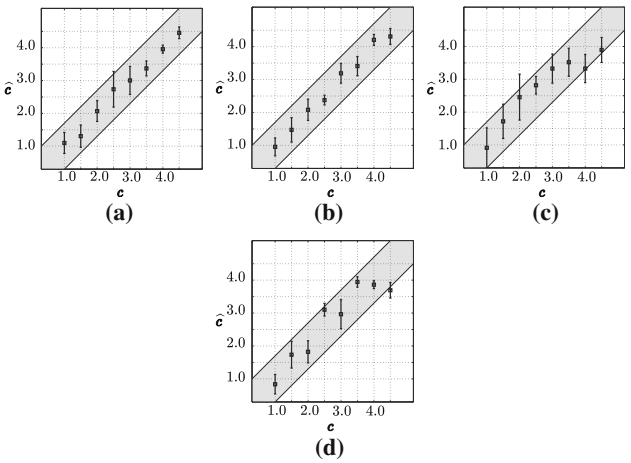

Fig. 11 Validation of the models for CRI database using leave-one-out cross validation procedure. Here $\hat{c}$ and c are automatic and human assessment, respectively. The *gray* strips in plots represent the error accepted by experts. **a** CRI-1, **b** CRI-3, **c** CRI-4, **d** CRI-6

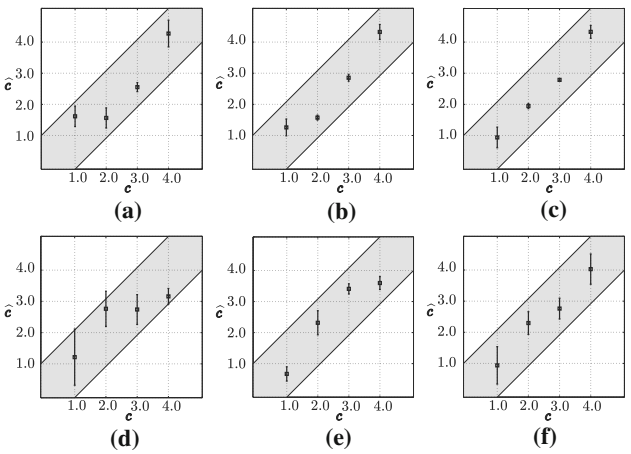

Fig. 12 Validation of the models for `EN1471` database using leave-one-out cross validation procedure. Here $\hat{c}$ and c are automatic and human assessment respectively. The *gray* strips in plots represent the error accepted by experts. **a** EN-A, **b** EN-B, **c** EN-C, **d** EN-D, **e** EN-G, **f** EN-H

with cut pile shag design, shows errors of labeling up to 1.5 in the worst case scenario. It means that the descriptors tested in this paper are not good enough for assessing wear degree in textile floor coverings with cut pile shag design. Then, it is necessary to include other kind of techniques, e.g., hairiness, for building accurate models. The errors of labeling for references DB1-3, DB1-7 and DB1-10 (Fig. 13b, e and g, respectively) are up to 1.0 in the worst case scenario. These results are not good enough according to the errors accepted by experts, labeling errors below 0.5. However, it brings a initial background to improve the process of measuring appearance retention in floor coverings. On the other hand, noteworthy is that the models for

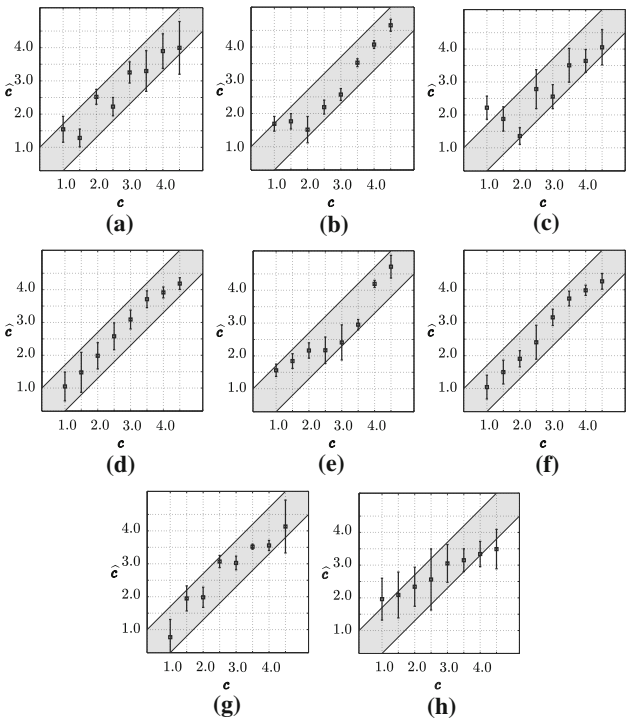

Fig. 13 Validation of the models for DB1 database using leave-one-out cross validation procedure. Here $\hat{c}$ and c are automatic and human assessment respectively. The *gray* strips in plots represent the error accepted by experts. **a** DB1-2, **b** DB1-3, **c** DB1-4, **d** DB1-5, **e** DB1-7, **f** DB1-9, **g** DB1-10, **h** DB1-16

references DB1-5 and DB1-9 (Fig. 13d, f, respectively) show labeling errors, in the worst case scenario, below 0.5 which is within the labeling error interval accepted by experts. This means that the degradation in textile floor coverings with loop pile construction can be characterized using only texture analysis.

5 Conclusions and future work

This paper has reviewed, selected and evaluated features in distinguishing fine changes of global texture. Particularly, we investigated the problem of appearance change in textile floor coverings due to degradation. The research was performed by following the conventional way of dividing the problem into a feature extraction stage, feature selection and classification stage. In the feature extraction stage we evaluated seventeen texture descriptors for characterizing changes in texture due to wear. We included descriptors based on statistics, filtering and models. We used two type of descriptors, one type computed from histograms and the other computed from data vectors. Then, the wear degree was quantified using descriptor differences between a reference sample and a degraded specimen. In this paper, those differences are used as

features or predictor variables. In the feature selection stage we designed a methodology for selecting features based on multiple regression analysis. Finally, in the classification stage, we used the conventional leave-one-out cross validation procedure to validate our methodology. The results showed that the power spectrum, local binary patterns, the texture spectrum, Gaussian Markov random fields, autoregressive models and the pseudo-Wigner distribution provide good descriptors in measuring appearance retention in floor coverings. Then, we believe that future work in distinguishing fine changes of global texture should be developed using those techniques.

Furthermore, a study of how the texture descriptors perform in changes of textile floor covering construction types was also presented. The results showed that textile floor coverings with *high pile* construction do not exhibit significative relationship between wear degree and the texture descriptors tested in this paper. Also, we proved that texture is an important descriptor in textile floor coverings with *low pile* construction. However, the degree of wear cannot be characterized using only texture unless the textile floor covering has loop pile construction. In such case, the linear combination between FFT and LBP is enough for measuring changes due to wear in textile floor coverings.

The study of complementary descriptors to texture for improving the process of measuring appearance retention in floor coverings remains as a future work. For instance, it is necessary to explore descriptors as hairiness, pilling, change of pattern definition, change in color, among others for improving the results presented in this paper. In addition, since the methodology is generic enough, it can be applied in any application in which a comparison between global textures is needed. For instance, in medical applications such as monitoring evolution of burned patients, texture changes in magnetic resonance imaging, evaluation of skin changes, among others. Also, it can be used in quality evaluation of still and/or image sequences in which a change of texture is seen as an artifact producing a change of quality. In general, this kind of methodology is very useful when it is necessary to compare two samples between them. Finally, we still need to study the impact of the feature selection methodology in classification results, i.e., to compare different feature selection methodologies within the proposed framework. Thus, it would be possible to measure the impact of feature selection in FCGT applications.

Acknowledgements This research is partially supported within the framework of WearTex project 2010−2011 funded by CWO; fellowship between Universiteit Gent, Universidad Antonio Nariño and Universidad Nacional de Colombia; and Universiteit Gent, iMinds,IPI. This work is partially supported by the project Universidad Nacional de Colombia, cod 20501007205.

References

1. Aibara T, Mabuchi T, Ohue K (1999) Automatic evaluation of the appearance of seam puckers on suits. In: Proceedings of the SPIE 3652, machine vision applications in industrial inspection VII, pp 1–4
2. Waegemana W, Cottyn J, Wyns B, Boullart L, De-Baets B, Van-Langenhove L, Detand J (2008) Classifying carpets based on laser scanner data. Eng Appl Artif Intell 21:907–918
3. Mirmehdi M, Xie X, Suri J (2008) Handbook of texture analysis, 1st edn. Imperial College Press, London
4. Zeuch N (2000) Understanding and applying machine vision, 2nd edn. Marcel Dekker, New York, pp 1–7
5. Siew LH, Hodgson RM, Wood EJ (1988) Texture measures for carpet wear assessment. IEEE Trans Pattern Anal Mach Intell 10:92–105
6. Davies S, Hall P (1999) Fractal analysis of surface roughness by using spatial data. J R Stat Soc Ser B (Stat Methodol) 61:3–37
7. Kang TJ, Kim SC, Sul IH, Youn JR, Chung K (2005) Fabric surface roughness evaluation using wavelet-fractal method part I: wrinkle, smoothness and Seam Pucker. Text Res J 75:751–760
8. Xie X (2008) A review of recent advances in surface defect detection using texture analysis techniques. Electron Lett Comput Vis Image Anal 7:1–22
9. Orjuela-Vargas S, Vansteenkiste E, Rooms F, De-Meulemeester S, De-Keyser R, Philips W (2010) Evaluation of the wear label description in carpets by using local binary pattern techniques. Text Res J 80:2132–2143
10. Xin W, Georganas ND, Petriu EM (2011) Fabric texture analysis using computer vision techniques. IEEE Trans Instrum Meas 60:44–56
11. Jose DJ, Hollies NRS, Spivak SM (1986) Instrumental techniques to quantify textural change in carpet part I: image analysis. Text Res J 56:591–597
12. Orjuela-Vargas S, Copot C, Syafiie S, Vansteenkiste E, Rooms F, Philips W, De-Keyser R, Van-Langenhove L (2008) Carpet wear classification using coocurrence matrices and support vector machines. In: Proceedings of the 19th annual workshop on circuits, systems and signal processing, pp 378–383
13. Orjuela-Vargas SA, Ortiz-Jaramillo B, Vansteenkiste E, Rooms F, De-Meulemeester S, de-Keyser R, Van-Langenhove L, Philips W (2012) Automatic grading of appearance retention of carpets using intensity and range images. J Electron Imaging. 21:021106
14. Mori T, Komiyama J (2002) Evaluating wrinkled fabrics with image analysis and neural networks. Text Res J 72:417–422
15. Mak KL, Li W (2008) Objective evaluation of Seam Pucker on textiles by using self-organizing Map. Int J Comput Sci 35:1–8
16. Saint-Marc P, Chen JS, Medioni G (1991) Adaptive smoothing: a general tool for early vision. IEEE Trans Pattern Anal Mach Intell 13:514–529
17. Wood EJ (1993) Description and measurement of carpet appearance. Text Res J 63:580–594
18. Palmer S, Zhang J, Wang X (2009) New methods for objective evaluation of fabric pilling by frequency domain image processing. Res J Text Appar 13:11–23
19. Pourdeyhimi B, Xu B, Nayernouri A (1994) Evaluating carpet appearance loss: Pile Lay orientation. Text Res J 64:130–135
20. Wang J, Wood EJ (1994) A new method for measuring carpet texture change. Text Res J 64:215–224
21. Xu B (1997) Quantifying surface roughness of carpets by fractal dimension. Cloth Text Res J 15:155–161
22. Jensen KL, Carstensen JM (2002) Fuzz and Pills evaluated on knitted textiles by image analysis. Text Res J 72:34–50
23. Choi CJ, Kim HJ, Jin YC, Kim HS (2009) Objective wrinkle evaluation system of fabrics based on 2D FFT. Fibers Polym 10:260–265

24. Mohri M, Hosseini-Ravandim SA, Youssefi M (2005) Objective evaluation of wrinkled fabric using radon transform. J Text Inst 96:365–370
25. Pourdeyhimi B, Xu B, Wehrle L (1994) Evaluating carpet appearance loss: periodicity and tuft placement. Text Res J 64:21–32
26. Militký J, Bleša M (2008) Evaluation of patterned fabric surface roughness. Indian J Fibre Text Res 33:246-252
27. Sun J, Yao M, Xu B, Bel P (2011) Fabric wrinkle characterization and classification using modified wavelet coefficients and support-vector-machine classifiers. Text Res J 81:902–913
28. Abril HC, Torres Y, Navarro R, Milln MS (1998) Automatic method based on image analysis for pilling evaluation in fabrics. J Opt Eng 37:2937–2947
29. Cristbal G, Hormigo J (1999) Texture segmentation through eigen-analysis of the Pseudo-Wigner distribution. Pattern Recognit Lett 20:337–345
30. Haralick RM (1979) Statistical and structural approaches to texture. Proc IEEE. 67:786–804
31. Swain MJ, Ballard DH (1990) Indexing via color histograms. In: Proceedings of the third international conference on computer vision, pp 390–393
32. Petrou M, Sevilla P (2006) Image processing: dealing with textures, 1st edn. Wiley, London
33. Heilbronner RP (1992) The autocorrelation function: an image processing tool for fabric analysis. Tectonophysics 212:351–370
34. Torabi A, Fossen H, Alaei B (2008) Application of spatial correlation functions in permeability estimation of deformation bands in porous rocks. J Geophys Res Solid Earth 113:1–10
35. Elunai R, Chandran V, Mabukwa P (2010) Digital image processing techniques for pavement macro-texture analysis. In: Proceedings of the 24th ARRB conference: building on 50 years of road transport research, pp 1–5
36. Chen CH, Pau LF, Wang PSP (1998) The handbook of pattern recognition and computer vision, 2nd edn. World Scientific Publishing Co., Singapore, pp 207–248
37. Randen T, Husy J (1999) Filtering for texture classification: a comparative study. IEEE Trans Pattern Anal Mach Intell 21:291–310
38. Unser M (1986) Sum and difference histograms for texture classification. IEEE Trans Pattern Anal Mach Intell 8:18–125
39. Lianantonakis M, Petillot YR (2005) Sidescan sonar segmentation using active contours and level set methods. Proc Europe Oceans 719–724
40. Menp T (2003) The local binary pattern approach to texture analysis extensions and applications. PhD thesis. University of Oulu
41. Dong Y, Ma J (2011) Wavelet-based image texture classification using local energy histograms. IEEE Signal Process Lett 18:247–250
42. Liu X, Wang D (2003) Texture classification using spectral histograms. IEEE Trans Image Process 12:661–670
43. Weszka JS, Dyer CR, Rosenfeld A (1976) A comparative study of texture measures for terrain classification. IEEE Trans Syst Man Cybern 6:269–285
44. Ade F (1983) Characterization of textures by Eigenfilters. Signal Process 5:451–457
45. Tkacenko A, Vaidyanathan PP, Nguyen TQ (2003) On the Eigenfilter design method and its applications: a tutorial. IEEE Trans Circuits Syst II Analog Digit Signal Process 50:497–517
46. Manjunath BS, Ma WY (1996) Texture features for browsing and retrieval of image Data. IEEE Trans Pattern Anal Mach Intell 18:837–842
47. Ortiz-Jaramillo B, Garcia-Alvarez J, Orjuela-Vargas S, Führ H, Castellanos-Dominguez G, Philips W (2012) Quantifying image distortion based on Gabor filter bank and multiple regression analysis. In: Procedings of the SPIE electronic imaging, conference 8293: image quality and system performance IX, 82930E
48. Burt PJ, Adelson EH (1983) The Laplacian pyramid as a compact image code. IEEE Trans Commun 31:532–540
49. Chan WY, Law NF, Siu WC (2003) Multiscale feature analysis using directional filter bank. In: Proceedings of the fourth international joint conference on information, communications and signal processing and the fourth Pacific rim conference on multimedia, pp 822–826
50. Vo A, Nguyen TT, Oraintara S (2006) Texture image retrieval using complex directional filter bank. In: Proceedings of the IEEE international symposium on circuits and systems, pp 5495–5498
51. Laws K (1980) Textured image segmentation. Technical report, University of Southern California Los Angeles Image Processing Inst
52. Suzuki MT, Yaginuma Y, Kodama H (2009) A 2D texture image retrieval technique based on texture energy filters. In: Proceedings of the international joint conference on computer vision, imaging and computer graphics theory and applications, pp 145–151
53. Lavvafi MR, Monadjemi S, Moallem P (2010) Film colorization, using artificial neural networks and laws filters. J Comput 5:1094–1099
54. Li S, Shawe-Taylor J (2005) Comparison and fusion of multiresolution features for texture classification. Pattern Recognit Lett 26:633–638
55. Heeger DJ, Bergen JR (1995) Pyramid-based texture analysis/synthesis. In: Proceedings of the 22nd annual conference on computer graphics and interactive techniques, pp 229–238
56. Areepongsa S, Park D, Rao K (2000) Invariant features for texture image retrieval using steerable pyramid. In: Proceedings of the 5th international symposium on wireless personal multimedia communications, pp 1–5
57. Mojsilovic A, Popovic MV, Rackov DM (2000) On the selection of an optimal wavelet basis for texture characterization. IEEE Trans Image Process 9:2043–2050
58. Redondo R, Fischer S, Sroubek F, Cristbal G (2008) A 2D Wigner distribution-based multisize windows technique for image fusion. J Vis Commun Image Represent 19:12–19
59. Joshi MS, Bartakke PP, Sutaone MS (2009) Texture representation using autoregressive models. In: Proceedings of the international conference on advances in computational tools for engineering applications, pp 386–390
60. Abbadeni N (2010) Texture representation and retrieval using the causal autoregressive model. Vis Commun Image Represent 21:651–664
61. Chen CC, Huang CL (1993) Markov random fields for texture classification. Pattern Recognit Lett 14:907–914
62. Paget R, Longsta D (1995) Texture synthesis via a non-parametric Markov random Field. In: Proceedings of the digital image computing: techniques and applications, pp 547–552
63. Yang F, Jiang T (2003) Pixon-based image segmentation with Markov random fields. IEEE Trans Image Process 12:1552–1559
64. Al-Kadi OS (2010) Texture measures combination for improved meningioma classification of histopathological images. Pattern Recognit 43:2043–2053
65. Zar J (2009) Biostatistical analysis, 5th edn. Prentice Hall, Englewood Cliffs
66. Thompson WR (2011) Variable selection of correlated predictors in logistic regression: investigating the diet-heart hypothesis. PhD thesis, Florida state university
67. Genizi A (1993) Decomposition of R^2 in multiple regression with correlated regressors. Stat Sin 3:407–420
68. Gan G, Ma C, Wu J (2007) Data clustering: theory, algorithms, and applications, 1st edn. ASA-SIAM

69. Cong G, Ma S (1996) Dyadic scale space. In: Proceedings of the 13th international conference on pattern recognition, pp 399–402
70. Garca S, Fernndez A, Luengo J, Herrara F (2010) Advanced nonparametric tests for multiple comparisons in the design of experiments in computational intelligence and data mining: experimental analysis of power. Inf Sci 180:2044–2064
71. Witten IH, Frank E, Hall MA (2011) Data mining: practical machine learning tools and techniques, 3rd edn. Morgan Kaufmann, Los Altos
72. Haralick RM, Shanmugam K, Dinstein I(1973) Textural features for image classification. IEEE Trans Syst Man Cybern 3:610–621
73. Wu Y, Pourdeyhimi B, Spivak SM, Hollies NRS (1990) Instrumental techniques to quantify textural and appearance changes in carpet part III: Colorimetric image analysis. Text Res J 60:673–687
74. Cant JS, Large ME, McCall L, Goodale MA (2008) Independent processing of form, color, and texture in object perception. Perception 37:57–78
75. Cavina-Pratesi C, Kentridge RW, Heywood CA, Milner AD (2010) Separate channels for processing form, texture, and color: evidence from fMRI adaptation and visual object agnosia. Cereb Cortex 20:2319–2332